

# Transition Temperature of a Magnetic Semiconductor with Angular Momentum $j$

Juana Moreno<sup>1</sup>, Randy S. Fishman<sup>2</sup>, and Mark Jarrell<sup>3</sup>

<sup>1</sup>Physics Department, University of North Dakota, Grand Forks, North Dakota 58202-7129

<sup>2</sup>Condensed Matter Sciences Division, Oak Ridge National Laboratory, Oak Ridge, Tennessee 37831-6032 and

<sup>3</sup>Department of Physics, University of Cincinnati, Cincinnati, Ohio 45221-0011

(Dated: November 20, 2018)

We employ dynamical mean-field theory to identify the materials properties that optimize  $T_c$  for a generalized double-exchange (DE) model. We reach the surprising conclusion that  $T_c$  achieves a maximum when the band angular momentum  $j$  equals  $3/2$  and when the masses in the  $m_j = \pm 1/2$  and  $\pm 3/2$  sub-bands are equal. However, we also find that  $T_c$  is significantly reduced as the ratio of the masses decreases from one. Consequently, the search for dilute magnetic semiconductors (DMS) materials with high  $T_c$  should proceed on two fronts. In semiconductors with  $p$  bands, such as the currently studied Mn-doped Ge and GaAs semiconductors,  $T_c$  may be optimized by tuning the band masses through strain engineering or artificial nanostructures. On the other hand, semiconductors with  $s$  or  $d$  bands with nearly equal effective masses might prove to have higher  $T_c$ 's than  $p$ -band materials with disparate effective masses.

The discovery of dilute-magnetic semiconductors (DMS) with current transition temperatures above  $170\text{ K}$  [1–3] initiated an active search for the optimal material for spintronic device applications [4]. However, the ferromagnetic transition temperature of magnetic semiconductors involves many parameters that are difficult to control experimentally. To facilitate the search for new magnetic semiconductors with high transition temperatures, we evaluate  $T_c$  for a double-exchange system with general angular momentum  $j$  using dynamical mean-field theory (DMFT). Surprisingly,  $T_c$  is found to reach a maximum for  $j = 3/2$  and for equal light and heavy hole masses. However, we also find that  $T_c$  decreases significantly when the ratio of the masses is reduced.

The notion of using magnetic semiconductors in spintronic devices dates back to the 1960's, when europium chalcogenides [5] and chromium spinels [6] were extensively studied. Before the appearance of the latest generation of III-V DMS grown by molecular beam epitaxy techniques [1, 2], II-VI [7] and IV-VI [8] DMS were developed by alloying non-magnetic semiconductors with magnetic ions. Improvement in growth techniques has pushed the  $T_c$  of  $\text{Ga}_{1-x}\text{Mn}_x\text{As}$  to values above  $170\text{ K}$  [3]. As we discuss later, the large value of  $T_c$  in delta-doped GaAs [9] might be associated with the reduced magnetic frustration when the Mn ions are restricted to two-dimensional planes.

In our calculation we employ the DMFT, which was formulated in the late 1980's by Müller-Hartmann [10] and Metzner and Vollhardt [11]. It has since developed into one of the most powerful many-body techniques for studying electronic models such as the Hubbard [12, 13] and DE [14–19] models. Since DMFT becomes exact in the dilute limit, it is a good starting point for studying DMS. Recent work on DMS materials has used DMFT to study variants of the DE model [20, 21] with less than one local moment per site. A DE model with one local moment per site and large coupling constant  $J_c$  provides an upper limit to the transition temperature for a system with exchange coupling between the local moments

and charge carriers. Perhaps more importantly, the behavior of  $n_h < x$  holes in the impurity band of a DMS with  $x < 1$  Mn atoms per site is very similar to that of a DE model with filling  $p = n_h/x < 1$  [21]. So as long as  $J_c$  is sufficiently large to produce a well-defined impurity band, the qualitative results of this model should be independent of the precise magnitude of  $J_c/W$  [19]. As we shall see, a generalized DE model with one local moment per site and large  $J_c$  also has the distinct advantage that analytic results are possible for any angular momentum  $j$  of the charge carriers.

In semiconductors like GaAs, the angular momentum of the holes is obtained from the vector sum of the  $s = 1/2$  spin with the  $l = 1$  orbital angular momentum of the  $p$  bands. The  $j = 3/2$  band lies highest in energy while the spin-orbit split  $j = 1/2$  band lies an energy  $\Delta_{so} \approx 340\text{ meV}$  below [22]. Consequently, almost all of the holes in Mn-doped GaAs populate the  $j = 3/2$  band, which in turn is split by crystal fields [23] into a  $m_j = \pm 3/2$  sub-band with heavy holes and a  $m_j = \pm 1/2$  sub-band with light holes. More exotic semiconductors with ( $l = 2$ )  $d$  bands, such as the chalcogenides [5], may contain carriers with total angular momentum  $j = 5/2$ .

The optimization of  $T_c$  is performed in two stages. First, we calculate  $T_c$  for a DE model where the charge carriers have angular momentum  $j$  but equal masses in all  $2j + 1$  sub-bands. After concluding that the system with  $j = 3/2$  and a half-filled lower or upper band has the highest  $T_c$ , we examine the effect of different band masses in the  $m_j = \pm 1/2$  and  $\pm 3/2$  sub-bands.

The Hamiltonian of a generalized DE model with carriers (holes or electrons) of angular momentum  $j$  and equal masses in all sub-bands is given by

$$H = \sum_{\mathbf{k}} \epsilon_{\mathbf{k}} c_{\mathbf{k}\alpha}^\dagger c_{\mathbf{k}\alpha} - \frac{J_c}{N} \sum_{i, \mathbf{k}, \mathbf{k}'} e^{i(\mathbf{k}-\mathbf{k}') \cdot \mathbf{R}_i} \mathbf{S}_i \cdot c_{\mathbf{k}'\alpha}^\dagger \vec{J}_{\alpha\beta} c_{\mathbf{k}\beta}, \quad (1)$$

where  $c_{\mathbf{k}\alpha}^\dagger$  and  $c_{\mathbf{k}\alpha}$  are the creation and destruction operators for an electron with angular-momentum component  $m_j = \alpha$  ( $\alpha = -j, -j+1, \dots, j$ ) and momentum  $\mathbf{k}$ ,

$\mathbf{S}_i = S\mathbf{m}_i$  is the spin of the local moment (treated classically) at site  $\mathbf{R}_i$ , and  $\vec{J}_{\alpha\beta}$  are the  $(2j+1)$ -dimensional angular-momentum matrices. Repeated spin indices are summed.

Within DMFT, the local effective action  $A_{\text{eff}}(\mathbf{m})$  is governed by the bare Green's function  $G_0$ , which contains dynamical information about the hopping of electrons onto and off neighboring sites. Because  $A_{\text{eff}}(\mathbf{m})$  is quadratic in the field variables, the full local Green's function  $G(i\nu_n)_{\alpha\beta}$  may be readily solved by integration, with the result [14]  $\underline{G}(i\nu_n) = \langle (\underline{G}_0(i\nu_n)^{-1} + \tilde{J}_c \underline{J} \cdot \mathbf{m})^{-1} \rangle_{\mathbf{m}}$ , where  $\nu_n = (2n+1)\pi T$  are Matsubara frequencies and underlined quantities are matrices in  $(2j+1) \times (2j+1)$  spin space;  $\langle X(\mathbf{m}) \rangle_{\mathbf{m}} = \int d\Omega_{\mathbf{m}} X(\mathbf{m}) P(\mathbf{m})$  denotes an average over the orientations  $\mathbf{m}$  of the local moment with a probability  $P(\mathbf{m})$ , and  $\tilde{J}_c = J_c S$ . This relation is solved for a semicircular density-of-states with full bandwidth  $W$  in terms of the electron filling  $p$  ( $p=1$  corresponds to one electron per site so that  $0 \leq p \leq 2j+1$ ) and the local-moment order parameter  $M = \langle m_z \rangle_{\mathbf{m}}$ , which becomes nonzero below  $T_c$ .

As  $\tilde{J}_c$  increases, the  $(2j+1)$ -degenerate band splits into  $2j+1$  sub-bands, each labeled by quantum number  $m_j$  and centered at energy  $-m_j \tilde{J}_c$ . Due to the effect of electronic correlations, the full bandwidth of each sub-band is lowered from  $W$  to  $W' = W/\sqrt{2j+1}$ . So prior to taking the limit of large  $J_c$  for the  $m_j$  sub-band, we must rewrite the chemical potential as  $\mu = -m_j \tilde{J}_c + \delta\mu$  where  $|\delta\mu| \leq W'/2$ .

Since matrix quantities like  $\underline{G}(i\nu_n)$ ,  $\underline{G}_0(i\nu_n)$ , and the self-energy  $\underline{\Sigma}(i\nu_n) = \underline{G}_0(i\nu_n)^{-1} - \underline{G}(i\nu_n)^{-1}$  have already been averaged over the orientations of  $\mathbf{m}$ , they are spin diagonal and may be expanded in powers of  $\underline{J}_z$  as  $\underline{A} = A_0 \underline{I} + A_1 \underline{J}_z + A_2 \underline{J}_z^2 + \dots$  where  $A_n$  is of order  $M^n$ . So to linear order in  $M$ , only the first two terms in this expansion are retained and the bare inverse Green's function may be parametrized as  $\underline{G}_0(i\nu_n)^{-1} = (z_n - m_j \tilde{J}_c + R_n) \underline{I} + Q_n \underline{J}_z$  where  $z_n = i\nu_n + \delta\mu$ .

For large  $J_c$  and to linear order in  $M$ , we solved self-consistent equations for  $R_n$  and  $Q_n$ . The Curie temperature satisfies the condition

$$\sum_n \frac{R_n^2}{R_n^2 - j(j+1)W'^2/16m_j^2} = 1, \quad (2)$$

while the filling  $p = T \sum_n \text{Tr} \text{Re}[\underline{G}(i\nu_n)] + j - m_j + \frac{1}{2}$ .

These two expressions generalize previous results [14, 18] for  $j = 1/2$ . Quite naturally, a system without partially filled sub-bands ( $p$  an integer) has a vanishing Curie temperature because the carriers are unable to hop to neighboring sites without incurring an infinite cost in coupling energy.

For a given  $j$ , the largest  $T_c$  always occurs in the sub-bands with  $m_j = \pm j$  because those holes or electrons are able to most effectively take advantage of the exchange coupling that mediates the ferromagnetism between the local moments. For  $j = 1/2, 3/2, 5/2, 7/2$ , and  $9/2$ , the

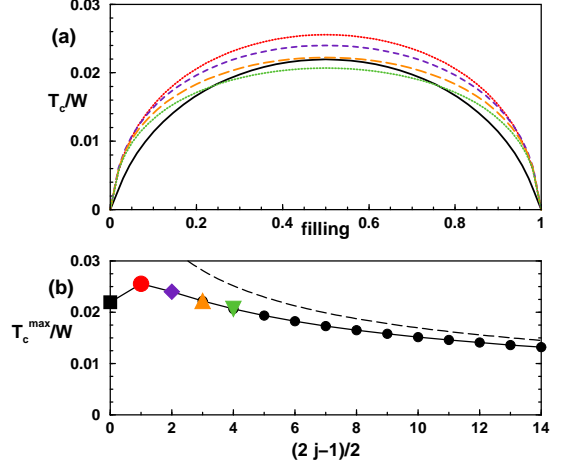


FIG. 1: Ferromagnetic transition temperature for a double-exchange model with general angular momentum  $j$ . (a) The dependence of  $T_c/W$  on filling for  $j = 1/2$  (solid black),  $3/2$  (dotted red),  $5/2$  (dashed purple),  $7/2$  (long-dashed orange), and  $9/2$  (dotted green). (b) The maximum transition temperature  $T_c^{\max}/W$  (in a half-filled band with  $m_j = \pm j$ ) versus  $(2j-1)/2$  with the limiting value  $1/(4\pi\sqrt{2j+1})$  plotted in the dashed curve. Large  $j$  values, although unphysical, are plotted to illustrate the asymptotic behavior.

dependence of  $T_c$  on filling within the  $m_j = \pm j$  sub-bands is plotted in Fig. 1(a). As expected,  $T_c$  is particle-hole symmetric within each sub-band and is the same for a system with  $p$  electrons ( $1-p$  holes) or  $p$  holes ( $1-p$  electrons) per site. So the largest Curie temperature,  $T_c^{\max}$ , is obtained when the lowest or highest sub-band is half-filled.

For a half-filled sub-band with  $m_j = \pm j$ , we obtain an analytic expression for  $T_c^{\max}$  by converting the Matsubara sum into an integral (assuming that  $T_c^{\max}/W$  is small), with the result

$$\frac{T_c^{\max}}{W} = \frac{1}{4\pi\sqrt{2j+1}} \left\{ 1 - \frac{1}{2\sqrt{j(j+1)}} \text{Tan}^{-1} \left( 2\sqrt{j(j+1)} \right) \right\}. \quad (3)$$

This expression gives a slightly larger value than the exact result obtained from Eq.(2), which is used to plot  $T_c^{\max}/W$  versus  $(2j-1)/2$  in Fig. 1(b). For large  $j$ ,  $T_c^{\max} \approx (W'/4\pi)\{1 - \pi/4j\}$  saturates at  $W'/4\pi$ , as indicated by the dashed line in Fig. 1(b). Compared to the maximum  $T_c^{\max}$  for  $j = 1/2$  of  $0.0219W$ ,  $T_c^{\max}$  for  $j = 3/2$  of  $0.0256W$  is 16% higher. Even systems with  $j = 5/2$  and  $7/2$  have higher  $T_c$ 's than one with  $j = 1/2$ . The suppression of  $T_c$  for  $j = 1/2$  is due to the stronger fluctuations at the smallest angular momentum.

To interpret Fig. 1(b), keep in mind that in the absence of magnetic impurities, a semiconductor is characterized by the bandwidth  $W$  of the conduction band and by the angular momentum  $j$  of the charge carriers. So for a class of undoped materials with the same bandwidth, the highest transition temperature will be found in the

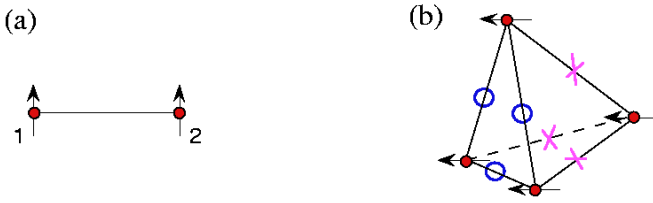


FIG. 2: Cartoon illustrating the magnetic frustration due to the chirality of the holes mediating the ferromagnetism. (a) The minimum energy configuration for a pair of Mn moments, (b) the frustration that occurs when 4 Mn atoms lie at the corners of a tetrahedron.

magnetic semiconductor with  $j = 3/2$ . A weakness of the present approach is that the local moments with spin  $S$  are treated classically whereas the charge carriers with angular momentum  $j$  are treated quantum-mechanically. Including the fluctuations of the local moments will further suppress  $T_c$ . Therefore, the optimum DMS system will have  $S \gg j$  so that fluctuations of the local moment can be neglected. This assumption is barely satisfied in Mn-doped GaAs, where  $S = 5/2$  [3].

Having established that the semiconductor with  $j = 3/2$  has the highest Curie temperature, we now examine the effect of different masses in the heavy  $m_j = \pm 3/2$  and light  $m_j = \pm 1/2$  sub-bands of the parent material. For GaAs, the band masses are  $m_h = 0.50m$  and  $m_l = 0.07m$  ( $m$  is the electron mass) with a ratio  $r = m_l/m_h = 0.14$  [22]. As pointed out by Zar  nd and Jank   [24], the different band masses introduce magnetic frustration because the kinetic energy  $K = \sum_{\mathbf{k},\alpha\beta} \epsilon_{\mathbf{k},\alpha\beta} c_{\mathbf{k},\alpha}^\dagger c_{\mathbf{k}\beta}$  is only diagonalized when the angular momentum of the charge carriers is quantized along the momentum direction (for  $r = 1$ , the quantization axis is arbitrary). Due to the chirality of the holes mediating the ferromagnetism, the moments of a pair of Mn atoms at sites  $\mathbf{R}_1$  and  $\mathbf{R}_2$  prefer to align perpendicular to the unit vector  $\mathbf{r}_{12}$  along the  $\mathbf{R}_2 - \mathbf{R}_1$  direction, as sketched in Fig. 2(a).

This anisotropy is easy to understand. Most of the carriers that couple Mn atoms 1 and 2 will have momentum  $\mathbf{k}$  along  $\mathbf{r}_{12}$  and angular momentum  $\mathbf{j}$  parallel to the Mn moments. If the Mn moments lie parallel to  $\mathbf{r}_{12}$ , only heavy holes with angular-momentum component  $\mathbf{j} \cdot \mathbf{r}_{12} = 3/2$  would couple the two Mn. But if the Mn moments lie perpendicular to  $\mathbf{r}_{12}$  as in Fig. 2(a), holes with angular momentum perpendicular to  $\mathbf{r}_{12}$  but momentum parallel to  $\mathbf{r}_{12}$  would contain all four angular-momentum components  $\mathbf{j} \cdot \mathbf{r}_{12} = \pm 3/2$  (heavy) and  $\pm 1/2$  (light). Due to the higher mobility of the light holes, the latter coupling is more effective. When four or more Mn atoms are distributed in space, the Mn interactions will be frustrated because some of the pairs cannot obtain their lowest energy configuration. This is shown schematically in Fig. 2(b), where the circles (crosses) indicate pairs of moments that are (not) in their minimum energy configurations. The large value of  $T_c$  in delta-doped

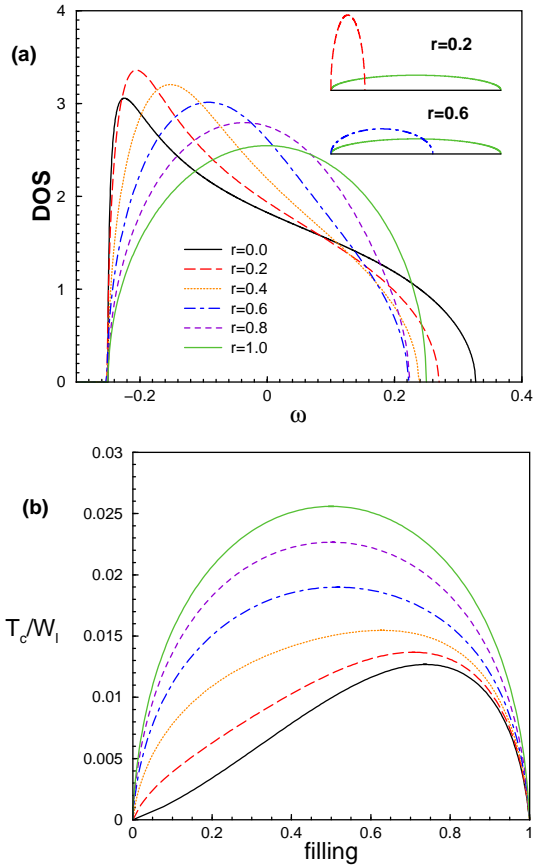


FIG. 3: Results for a double-exchange model with  $j = 3/2$  and different carrier masses in the heavy and light sub-bands. (a) The interacting density-of-states for  $j = 3/2$  and a range of ratios  $r$  between the effective masses; at the right hand corner the non-interacting densities-of-states for  $r = 0.2$  and  $0.6$ . (b) The dependence of  $T_c/W_l$  on filling for  $j = 3/2$  and the same values of  $r$ .

GaAs [9] may be related to the reduced magnetic frustration when Mn ions restricted to two-dimensional planes can order with their moments perpendicular to the plane.

The calculation of  $T_c$  is performed using two semi-circular densities-of-states such as the ones sketched in the right hand corner of Fig. 3(a) with bandwidths  $W_l$  and  $W_h = rW_l$ . As the interaction  $J_c$  is turned on, the interacting density-of-states separates into four identical sub-bands which are *not* particle-hole symmetric. In Fig. 3(a), we plot one of these sub-bands for a range of effective mass ratios  $r$ . For  $r < 1$ , the interacting density-of-states is always weighted towards lower energies, where the heavy holes dominate.

In Fig. 3(b), we plot  $T_c/W_l$  versus filling for the same values of  $r$  used in Fig. 3(a). Not surprisingly,  $T_c$  decreases as  $r$  decreases from 1 due to the magnetic frustration introduced by the chirality of the charge carriers. Hence, the maximum  $T_c$  for a fixed light bandwidth is obtained when the band masses are identical.

As  $r$  drops from 1 to 0,  $T_c^{\max}/W_l$  plotted in Fig. 4

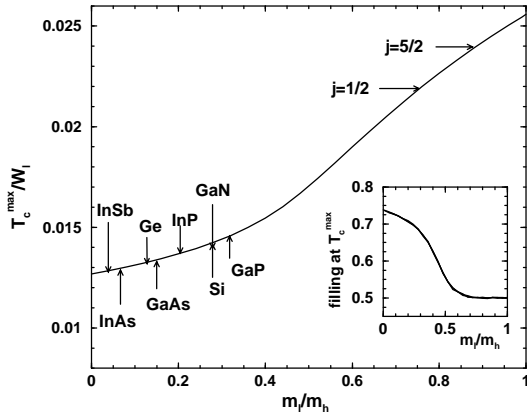


FIG. 4: Relation between  $T_c^{\max}$  and the ratio of effective masses  $r = m_l/m_h$ . In the main panel,  $T_c^{\max}/W_l$  is plotted versus  $r = m_l/m_h$ , with the experimental ratios denoted for several semiconductors. The horizontal arrows denote  $T_c^{\max}/W_l$  for  $j = 1/2$  and  $j = 5/2$  (equal masses in all sub-bands). The inset displays the filling for which the largest  $T_c$  is obtained versus  $m_l/m_h$ .

decreases by 50% from 0.0256 to 0.0127. For the experimental value  $r = 0.14$  [22],  $T_c^{\max} \approx 0.0133W_l$  has decreased 48% from its unfrustrated value. The experimental parameters  $r$  for a variety of semiconductors with  $j = 3/2$  are also indicated in Fig. 4. Based on numerical results with Mn concentration  $x < 1$  [21], however, the suppression of  $T_c$  may not be quite so dramatic as suggested by this figure. Notice also that a system with  $j = 1/2$  or  $j = 5/2$  and nearly identical band masses may have a higher transition temperature than one with  $j = 3/2$  but very different effective carrier masses.

In the inset to Fig. 4, we plot the filling at which  $T_c$  is maximized versus the ratio of masses. This filling varies

from  $p = 0.5$  at  $r = 1$  to roughly 0.74 at  $r = 0$ . So for  $r < 1$ , the transition temperature is no longer particle-hole symmetric within the lowest sub-band. This may explain why the transition temperature in Mn-doped GaAs continues to increase for hole fillings supposedly larger than half of the Mn doping [25, 26]. Based on this work, we expect that  $T_c$  reaches a maximum for a filling close to 70%.

To summarize, we have examined the general dependence of the transition temperature of a magnetic semiconductor on the angular momentum and filling of the charge carrier bands. For a fixed bandwidth of the parent compound,  $T_c$  is maximized when  $j = 3/2$ , the same angular momentum carried by the holes in GaAs and Ge. For  $j > 3/2$ , the angular momentum of the charge carriers effectively suppresses  $T_c$  due to the narrowing of the impurity band by electronic correlations. However, the suppression of  $T_c$  due to the different effective masses in  $p$ -band semiconductors is even more significant. Because of the strong reduction of  $T_c$  by the magnetic frustration,  $s$ -band ( $j = 1/2$ ) or  $d$ -band ( $j = 5/2$ ) semiconductors with more nearly equal band-masses may prove to have higher  $T_c$ 's than  $p$ -band ( $j = 3/2$ ) semiconductors with disparate effective masses. For the class of  $j = 3/2$  semiconductors,  $T_c$  will be maximized when the effects of magnetic frustration are reduced as much as possible. This may be achieved either by applying strain, thereby altering the band structure, or through digital doping [9].

We gratefully acknowledge useful conversations with Horacio Castillo, Paul Kent and Igor Žutić. This research was sponsored by the U.S. Department of Energy under contract DE-AC05-00OR22725 with Oak Ridge National Laboratory, managed by UT-Battelle, LLC and by the National Science Foundation under Grant Nos. DMR-0312680 and EPS-0132289 (ND EPSCOR).

---

[1] H. Ohno, A. Shen, F. Matsukura, A. Oiwa, A. Endo, S. Katsumoto and Y. Iye, *Appl. Phys. Lett.* **69**, 363 (1996).

[2] H. Munekata, H. Ohno, S. von Molnár, Armin Segmüller, L.L. Chang, and L. Esaki, *Phys. Rev. Lett.* **63**, 1849 (1989).

[3] For a recent review: A. H. MacDonald, P. Schiffer, and N. Samarth, *Nature Materials* **4**, 195 (2005).

[4] I. Žutić, J. Fabian, S. Das Sarma, *Rev. Mod. Phys.* **76**, 323 (2004).

[5] A. Mauger and C. Godart, *Phys. Rep.* **141**, 51 (1986) and reference therein.

[6] P. K. Baltzer, P. J. Wojtowicz, M. Robbins, and E. Lopatin, *Phys. Rev.* **151**, 367 (1966).

[7] J. K. Furdyna and J. Kossut (Eds.), *Semiconductors and semimetals*, Volume **25**, Academic Press, San Diego (1988).

[8] T. Story, R. R. Galazka, R. B. Frankel and P. A. Wolff, *Phys. Rev. Lett.* **56**, 777 (1986).

[9] A. M. Nazmul, S. Sugahara, and M. Tanaka, *Phys. Rev. B* **67**, 241308(R) (2003).

[10] E. Müller-Hartmann, *Z. Phys. B* **74**, 507 (1989); E. Müller-Hartmann, *Z. Phys. B* **76**, 211 (1989).

[11] W. Metzner and D. Vollhardt, *Phys. Rev. Lett.* **62**, 324 (1989).

[12] J.K. Freericks and M. Jarrell, *Phys. Rev. Lett.* **74**, 186 (1995).

[13] Applications of DMFT to the Hubbard model and additional references are contained in the comprehensive review article: A. Georges, G. Kotliar, W. Krauth, and M.J. Rozenberg, *Rev. Mod. Phys.* **68**, 13 (1996).

[14] N. Furukawa, *J. Phys. Soc. Jpn.* **64**, 2754 (1995); N. Furukawa, *J. Phys. Soc. Jpn.* **64**, 3164 (1995).

[15] A.J. Millis, R. Mueller, and B.I. Shraiman, *Phys. Rev. B* **54**, 5389 (1996); *ibid.* **54**, 5405 (1996).

[16] B. Michaelis and A.J. Millis, *Phys. Rev. B* **68**, 115111 (2003).

[17] M. Auslender and E. Kogan, *Phys. Rev. B* **65**, 012408 (2001); M. Auslender and E. Kogan, *Europhys. Lett.* **59**, 277 (2002).

[18] R.S. Fishman and M. Jarrell, *J. Appl. Phys.* **93**, 7148

(2003); R.S. Fishman and M. Jarrell, Phys. Rev. B **67**, 100403 (2003).

[19] A. Chernyshev and R.S. Fishman, Phys. Rev. Lett. **90**, 177202 (2003).

[20] A. Chattopadhyay, S. Das Sarma, and A.J. Millis, Phys. Rev. Lett. **87**, 227202 (2001).

[21] K. Arayannpour, J. Moreno, M. Jarrell, and R.S. Fishman, Phys. Rev. B (in press).

[22] J.S. Blakemore, J. Appl. Phys. **53**, R123 (1982).

[23] J.M. Luttinger and W. Kohn, Phys. Rev. **97**, 869 (1955).

[24] G. Zaránd and B. Jankó, Phys. Rev. Lett. **89**, 047201 (2002).

[25] K. C. Ku, S. J. Potashnik, R. F. Wang, S. H. Chun, P. Schiffer, N. Samarth, M. J. Seong, A. Mascarenhas, E. Johnston-Halperin, R. C. Myers, A. C. Gossard, and D. D. Awschalom, Appl. Phys. Lett. **82**, 2302 (2003).

[26] K. W. Edmonds, K. Y. Wang, R. P. Campion, A. C. Neumann, N. R. S. Farley, B. L. Gallagher, and C. T. Foxon, Appl. Phys. Lett. **81**, 4991 (2002).